Molecular dynamics simulation study of binary fullerene mixtures

R. Ruberto, M. C. Abramo,* and C. Caccamo
Istituto Nazionale per la Fisica della Materia (INFM) and Dipartimento di Fisica Università di Messina, Contrada Papardo, C.P. 50-98166 Messina, Italy

(Received 28 July 2004; published 26 October 2004)

We report constant-pressure molecular dynamics (MD) simulations of binary C_{60}/C_n fullerene-mixtures ($n=70$, 76, 84, 96) modeled in terms of a spherically symmetric two-body potential. By starting from a liquid configuration of the system, we cool mixtures down to freezing and beyond, until room temperature is reached, in order to verify the formation of solid solutions, namely, of configurations characterized by a unique crystalline lattice whose sites are randomly occupied by the two component fullerene species. We first explore the entire concentration range of the $C_{60x}/C_{70(1-x)}(0<x<1)$ mixture and find fairly good agreement with experimental data, exhibiting partial reciprocal solubility of the two components into each other with an immiscibility gap at intermediate compositions. In fact, the system we simulate forms substitutional solid solutions over a wide range of concentrations except for $0.3\leqslant x\leqslant 0.5$; over such an interval, it turns out that the initially liquid mixture can be supercooled down to relatively low temperatures, until eventually a glassy phase is formed. The study is then extended to fullerene mixtures of molecular diameter ratio $\alpha=\sigma_{C_{60}}/\sigma_{C_n}$ smaller than in C_{60}/C_{70} (where $\alpha=0.93$), as is the case for C_{60}/C_{76} ($\alpha=0.89$), C_{60}/C_{84}($\alpha=0.85$) and C_{60}/C_{96} ($\alpha=0.79$). The effect of the size mismatch between the two species is dramatic: The solid immiscibility region rapidly expands even upon a tiny reduction of α, with formation of an amorphous phase at sufficiently low temperature, as found for the C_{60}/C_{70} mixture. For the smallest $\alpha(C_{60}/C_{96})$ cocrystallization of the two components turns out to be forbidden over the whole concentration axis. A mapping of the MD evidences of the fullerene mixtures' phase behavior onto the phase diagram of binary hard-sphere mixtures (determined by other authors) turns out to be worthwhile and enlightening. In particular, size ratio effects and the onset of glassy phases emerge in qualitative good agreement with such studies, and with results of phase coexistence calculations in model binary colloidal systems.

DOI: 10.1103/PhysRevB.70.155413 PACS number(s): 61.48.+c, 64.75.+g, 64.70.Dv, 64.70.Pf

I. INTRODUCTION

Most of the scientific investigation on fullerenes has been carried out on pure materials, especially C_{60} and C_{70}. Conversily, the number of studies concerning fullerene mixtures is comparatively much smaller, although such substances are often condensed together, and an understanding of the physical properties of the resulting multicomponent system would be very useful. We quote in this instance recent investigations which have been carried out on solid solutions of fullerenes, revealing interesting features. For instance, a nonadditive behavior in the photoluminescence spectra of C_{60}—C_{70} solid mixtures has been reported by Sauvajol *et al.*;[1] Tanaka *et al.*[2] have investigated the suppression of the Curie temperature of TDAE-C_{60} containing C_{70} as impurity, while McGhie *et al.* and Zielinski *et al.* have showed that C_{60} impurities in solid C_{70} substantially depress the orientational transition temperatures and enthalpies.[3]

A still open question in mixed fullerene investigation concerns the possibility to form substitutional solid solutions of C_{60} and C_{70}, in any concentration ratio. Baba *et al.*[4] have investigated this point by measuring through Knudsen effusion mass spectrometry, the partial pressures of the two fullerenes in the temperature range (600-800 K) and for several compositions of the mixture. Their results suggested that C_{60} and C_{70} are soluble into each other in the solid state to the extent of about 30%, with a miscibility gap between these two extreme concentration regimes. Kniaz *et al.*[5] reported differential scanning calorimetry and powder x-ray diffraction data for C_{60x}-$C_{70(1-x)}$ $(0<x<1)$ fullerene alloys; they found that dilute samples prepared from toluene solution exhibit the very large miscibility gap $0.04<x<0.95$, whereas alloys prepared by sublimation are miscible in all proportions. Havlik *et al.*[6] showed results that are in favor of Baba's hypothesis, for samples prepared by controlled condensation from the vapor phase.

As far as theoretical studies of fullerene mixtures are concerned, we are able to quote only a Monte Carlo (MC) calculation of the structural properties of a 50% C_{60}—C_{70} alloy, based on a Lennard-Jones potential representation of the interaction between C_{60} and C_{70} molecules,[7] predicting a solid solution for this particular concentration.

We now observe in this connection that another model potential, due to Girifalco,[8] is currently in use for the theoretical investigation of fullerenes. This model is based on the fact that in crystalline C_{60} the molecular cages are orientationally disordered and freely rotate for temperatures $T>260$K; this circumstance allows one to describe the interaction between two fullerenes in terms of an analytic spherically symmetric pair potential. The availability of such an explicit functional form for the molecular interaction has obviously been advantageous in several respects, in particular in order to make feasible extensive simulations of C_{60} and to map out its phase diagram.[9]

Now, recent studies suggest that a similar "smeared out" spherical description can be attempted for $C_{n>60}$ molecules

although some of these can have a sensibly nonspherical shape: the cases $n=70$, 76, 84, and 96 have in particular been examined.[10–13]

In this work, we report extensive constant pressure molecular dynamics (MD) simulations of C_{60}—C_{70} fullerene mixtures, at temperatures which in any case are high enough that both the two pure components are orientationally disordered so to allow the adoption of the Girifalco model.

All mixtures are deeply cooled by starting from a liquid configuration of the system in order to investigate the solid phases obtained at freezing. We test in this manner the possible existence of solid solutions against miscibility gaps, as well as the formation of glassy phases. We then study size ratio effects, by extending the previously described cooling procedure to binary fullerene mixtures characterized by a molecular diameter ratio smaller than in C_{60}/C_{70}, such as C_{60}/C_{76}, C_{60}/C_{84}, and C_{60}/C_{96}.

We note that, due to the steeply repulsive nature of the Girifalco potential, one can assume that hard sphere mixtures (HSM) can serve as a reference system for the mixed fullerenes. HSM have been extensively studied in recent years, as a realistic model of colloidal suspensions, protein solutions, and other complex fluids; in particular, the phase diagram of binary HSM has been calculated through density functional theory (DFT)[14–16] and MC simulations.[17] Now, as we shall show, a close similarity emerges between the phase behavior of mixed fullerenes versus that of HSM. It will appear, in particular, that the two "bucky-ball" species may not form solid solutions in all proportions and that an intermediate concentration region exists of solid immiscibility which expands upon reduction of the diameter ratio, as indeed is found in HSM[14–17]

We shall also show that the concentration interval of solid phase immiscibility is the same over which the mixture remains liquid down to rather low temperatures, by eventually yielding a glassy phase. This behavior is typically encountered in phase diagrams characterized by a deep eutectic as colloidal mixtures,[18] polystirene sphere mixtures,[19] and metallic alloys.[20] In particular, we shall point out in some detail the analogies emerging between our results and those reported in Ref. 18 for binary colloidal hard spheres.

We describe in Sec. II the model and the computational strategy adopted. Section III is devoted to the results and discussions. The conclusions follow in Sec. IV.

II. MODEL AND COMPUTATIONAL METHOD

A generalization of the basic Girifalco expression for the interaction potential between two C_{60} molecules, to the case of a fullerene mixture has been obtained by Kniaz *et al.*[5] and reads

$$v_{ij}(r) = -\frac{N_i N_j A}{48 d_i d_j r}\left[\frac{1}{[r-(d_i+d_j)]^3} - \frac{1}{[r+(d_i-d_j)]^3} - \frac{1}{[r-(d_i-d_j)]^3} + \frac{1}{[r+(d_i+d_j)]^3}\right] + \frac{N_i N_j B}{36 d_i d_j r}\left[\frac{1}{[r-(d_i+d_j)]^9} - \frac{1}{[r+(d_i-d_j)]^9} - \frac{1}{[r-(d_i-d_j)]^9} + \frac{1}{[r+(d_i+d_j)]^9}\right]. \quad (1)$$

N_i and d_i stand for the number of C atoms and the radius of the ith fullerene species, respectively. We shall also use in what follows the notation $\sigma_i = 2d_i$ to indicate the ith fullerene species diameter. A and B are the parameters entering the 12-6 potential $v_{CC} = -A/r^6 + B/r^{12}$ through which two carbon atoms placed on different molecular cages are assumed to interact. Equation (1) is then obtained by integrating this potential over two facing spherical cages of radius d_i and d_j, respectively, by assuming a continuous distribution of carbon interaction sites over the two molecular surfaces.

In what follows we shall consider mixtures of C_{60} with C_{70}, C_{76}, C_{84}, and C_{96}, by describing the intermolecular interaction in terms of potential (1). To this aim we first fix A and B for all the systems investigated to the values originally determined by Girifalco for pure C_{60}, namely, $A = 32.0 \times 10^{-60}$ erg cm^6 and $B = 55.77 \times 10^{-105}$ erg cm^{12}. The C_{60} diameter is also taken according to Ref. 8, namely, $\sigma_{C_{60}} = 0.71$ nm. As far as the diameters of the other fullerene molecules are concerned, we make reference to previous papers by us[10–12] and another author,[13] in which the Girifalco potential has been adapted to nonspherical molecules, as C_{70} and C_{76}. Specifically, in Ref. 10 the diameter of the C_{70} fullerene cage is fixed by fitting, through MD simulation, the lattice parameter of the C_{70} fullerite crystal at room temperature (RT). A similar procedure has been employed in Ref. 12 in order to fix the diameter of C_{76} and C_{84}. As for C_{96}, we adopt a simple geometrical rule of Refs. 11 and 13 by which the molecular diameter is assumed to scale with the number of carbon atoms. Table I summarizes the relevant potential parameters which we shall use in simulating the different mixtures, while a comprehensive representation of the full potential patterns is offered in Figs. 1 and 2.

We shall further characterize each mixture by the size ratio

$$\alpha = \frac{\sigma_{C_{60}}}{\sigma_j}$$

of the smaller C_{60} to the bigger jth molecule species, with $j = C_{70}$, C_{76}, C_{84}, C_{96}, and the concentration

$$x = \frac{\rho_j}{\rho_{C_{60}} + \rho_j},$$

where ρ_j is the number density of particles of the jth species. In our study we examine mixtures with four different α's (see Table I) at eleven different compositions ($x = 0.0$, 0.125, 0.25, 0.333, 0.4, 0.5, 0.6, 0.667, 0.75, 0.875, and 1.0). Thermodynamic, static, and dynamical properties of the model mixtures are obtained by means of constant pressure MD simulation in the N-P-T ensemble.

Starting from a simple cubic lattice of 1000 molecules of C_{60}, we prepare a binary solid system by randomly replacing these particles with molecules of species j in x proportion. Such mixed crystalline configuration is first melted at $T = 2000$ K and $P = 3.5$ MPa, by verifying through the analysis of structural and dynamical quantities that a fully liquid state

TABLE I. Parameters characterizing the simulation potential $v_{ij}(r)$ for like (top) and unlike (bottom) interaction. R_0 is the point of zero potential; ϵ/k_B is the minimum depth in K; distances are expressed in nanometers.

	C_{60}	C_{70}	C_{76}	C_{84}	C_{96}
σ_{C_n}	0.71	0.762	0.7949	0.8307	0.8991
R_0	0.959	1.011	1.043	1.079	1.147
$-\epsilon/k_B$	3218	3653	3853	4203	4456
		C_{60}/C_{70}	C_{60}/C_{76}	C_{60}/C_{84}	C_{60}/C_{96}
α		0.93	0.89	0.85	0.79
R_0		0.985	1.015	1.019	1.053
$-\epsilon/k_B$		3429	3523	3672	3773

is effectively achieved. The liquid mixture is then progressively cooled through different cooling rates (CR), most of the calculations having been performed by imposing a 30 K decrease over 20 000 MD steps (CR1), with a time-step equal to 5.0×10^{-15} s. Averages are then cumulated over successive 10 000 steps. This sequence is iterated until RT is reached. An order of magnitude smaller cooling rate (CR2), consisting in imposing a 30 K decrease over 200 000 MD steps, is also adopted for all the mixtures envisaged at equimolar concentration. Averages are cumulated after cooling, through the same procedure as in the CR1 case. The CR2 sequence is also iterated several times, until temperatures as low as 600 K, or similar, are reached. We did not attain RT in this case: in fact, the computational time involved is quite demanding while, on the other hand, the evolution of the system in the glassy phase appears unambiguously attained much earlier than RT is reached.

III. RESULTS AND DISCUSSION

A. C_{60}/C_{70} fullerene mixtures

C_{60}/C_{70} mixtures (α=0.93), are first cooled through the cooling rate CR1.

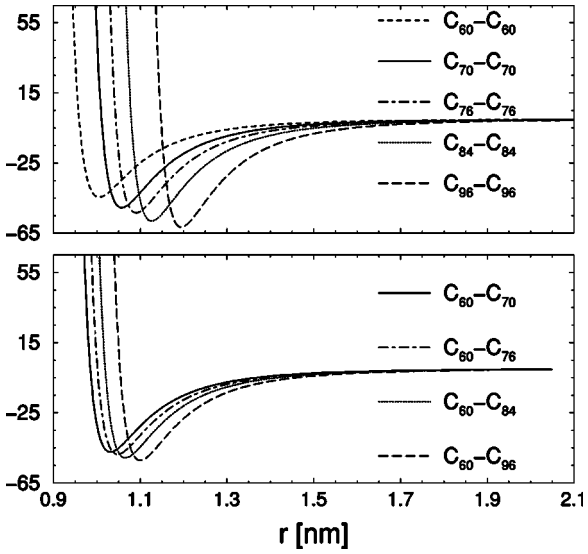

FIG. 1. Like (top) and unlike (bottom) fullerene-fullerene interaction in absolute distance and energy units.

It emerges that the system undergoes crystallization at all concentrations with the exception of the range $0.3\leqslant x\leqslant0.5$. Crystallization takes place by forming a highly defective fcc structure with lattice sites occupied at random by the two fullerene species. The crystallization process is clearly documented by either a marked drop, or change of slope, in the volume and enthalpy versus temperature patterns (see Figs. 3 and 4). Evidence of the crystallizations also comes from the modifications (not shown here) in the radial distribution functions (rdfs) with the decreasing temperature. One can observe, in fact, a gradual heralding of the peaks in the $g_{ij}(r)$ patterns, at positions which correspond to the typical distances of the fcc lattice. It also emerges from the same rdfs' evolution, as well as from snapshots of the cooled system, that crystallization starts from the majority component of the mixture, to involve later the minority one. A dynamical analysis also documents crystallization, since we find that the diffusion coefficients experience marked changes of slopes at the transition temperature, by eventually attaining values as low as 10^{-8} cm^2/s, three orders of magnitude below the value typical of the fluid regime.

After the transition, the system is further cooled down to RT. The final form thereby attained by the rdfs is shown in Fig. 5.

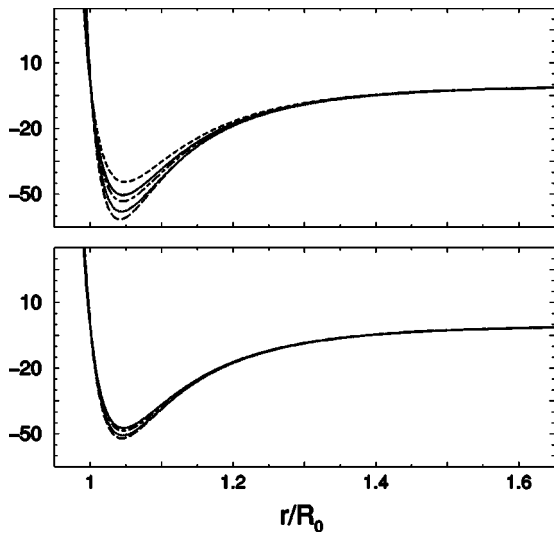

FIG. 2. Fullerene—fullerene interaction as in Fig. 1, in reduced distance units.

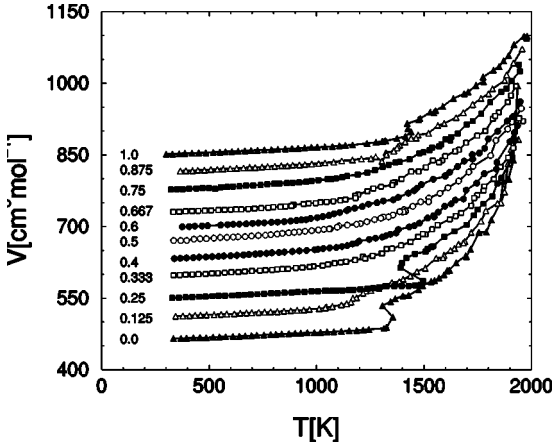

FIG. 3. Volume of the C_{60}/C_{70} mixtures versus temperature at different C_{70} concentrations, appearing as labels beside the curves.

As far as the variation of the crystallization temperature with the composition of the mixture is concerned, it initially decreases with increasing the percentage of C_{70}, as shown in Table II. At $x=0.25$, however, the two components crystallize simultaneously, at a temperature sensibly higher than what found at $x=0.125$. Also note that, as shown in Fig. 6 (top), where RT density values versus x are reported, the density initially decreases with the increase of the C_{70} concentration, an effect obviously due to the volume expansion of the system induced by the insertion of the bigger C_{70} molecules. At $x=0.25$, however, this trend is inverted, a result which we attribute to a most efficient packing of the spheres for the given size ratio. Indeed, structural features are consistent with such a picture since the rdfs exhibit at this concentration more pronounced peaks than elsewhere. A similar situation emerges at $x=0.667$, where the crystallization temperature shows another relative maximum (see Table II), and more peaked rdfs. Enthalpy data complement significantly this picture. In fact, as we can observe in Fig. 6 (bottom), enthalpy displays two minima in correspondence of the density maxima, while it shows a kind of "plateau" of comparitevely higher values, in the intermediate concentration regime. This latter feature appears consistent with the formation of amorphous phases as we are going to discuss immediately below.

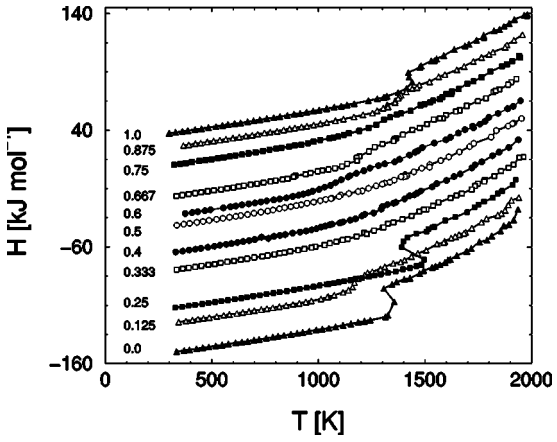

FIG. 4. Same as Fig. 3 for the enthalpy of the C_{60}/C_{70} mixtures.

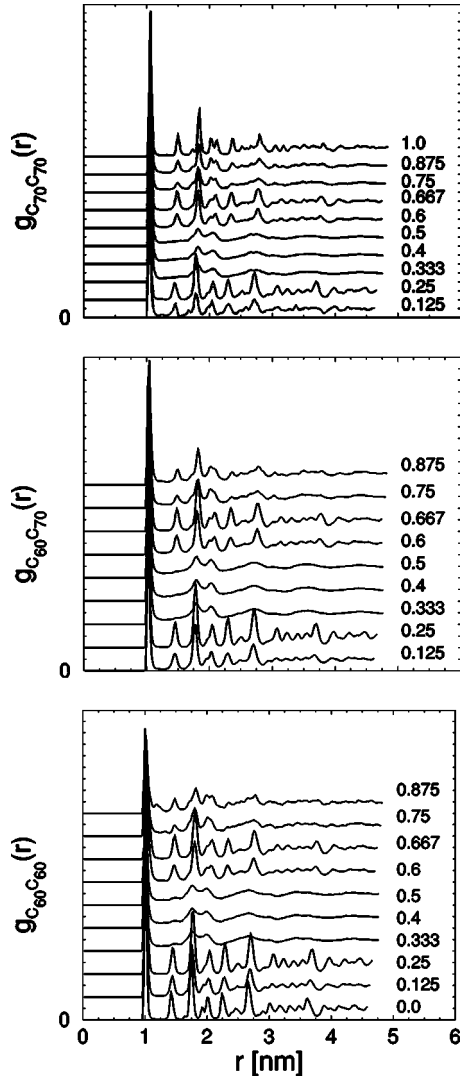

FIG. 5. Room temperature rdfs. of the C_{60}—C_{70} solid solutions at different concentrations (labeling the curves). Rdfs. are displayed shifted by two units on the ordinate axis.

We can argue from all these data that two specific concentrations exist, one on the C_{60}-and the other on the C_{70}-rich end, at which RT solid solutions is particularly favored.

The system exhibits a substantially different behavior in the concentration range $0.3 \leqslant x \leqslant 0.5$. Mixtures of such compositions, when cooled through CR1, eventually attain a "frozen" solidlike state, lacking periodicity, in a configuration which has the characteristics of a glass. This is documented by: (i) the occurrence of a splitted second peak in the rdfs at $x=0.333$, 0.4, and 0.5 (see Fig. 5), a feature typically associated to the formation of an amorphous phase, and by the absence of other peaks at distances proper of the fcc arrangement, clearly visible instead in the other $g_{ij}(r)$ patterns; and (ii) the changes of slopes in the volume and enthalpy versus T patterns at the concentration of interest, visible in Figs. 3 and 4; (iii) the change of slope of the diffusion coefficient D (not shown here); and (iv) the snapshots of the

TABLE II. Parameters characterizing the onset of the crystallization in the C_{60}/C_n fullerene mixtures. Crystallization temperatures are reported in absolute $[T_c]$ and reduced units $[T_c^*=k_BT_c/\epsilon]$. Values of the crystallization densities (ρ_c) and total packing (η_c) (see text for the definition) are also shown.

x	T_c [K]	T^*	ρ_c[nm^{-}3]	η_c
		C_{60}/C_{70}		
0.0	1307	0.4000	1.124	0.5470
0.125	1217	0.3549	1.131	0.5686
0.25	1391	0.4056	1.087	0.5598
0.6	1213	0.3537	1.068	0.5869
0.667	1357	0.3957	1.031	0.5825
0.75	1307	0.3811	1.025	0.5890
0.875	1388	0.4047	0.999	0.5880
1.0	1422	0.3890	0.9747	0.5880
		C_{60}/C_{76}		
0.125	1282	0.3638	1.104	0.555
0.875	1406	0.4000	0.929	0.6
1.0	1497	0.3880	0.884	0.598
		C_{60}/C_{84}		
0.875	1506	0.4101	0.850	0.6
1.0	1579	0.3760	0.812	0.6
		C_{60}/C_{96}		
1.0	1693	0.3790	0.676	0.6

system at RT confirming that amorphous phases are effectively formed at different concentrations in the range $0.3 \leqslant x \leqslant 0.5$.

It is worth noting at this stage that, as it has been recently documented by us,[21] a high temperature glass transition takes place also in the Girifalco model of pure C_{60}. The transition, evidentiated during fast quenching in constant pressure MD of the liquid C_{60} phase, is totally distinct from the orientational glass transition taking place in real life C_{60} at 90 K,[22] and occurs at 1100 *K* for a pressure of 3.5 MPa. The adoption instead of a cooling rate identical to CR1 for such a pure case invariably leads to crystallization.[21] It thus appears that there is an easiness for glass formation in the mixed fullerene case which, as we shall discuss in detail below, crucially depends both on the relative concentration and the size ratio of the component species.

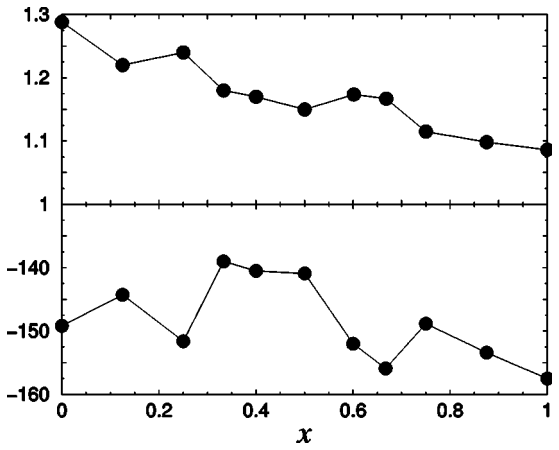

FIG. 6. RT density (top) and enthalpy (bottom) of the C_{60}—C_{70} mixtures.

It is now interesting to examine the system behavior immediately before the glass phase is formed. It appears that in the range $0.3 \leqslant x \leqslant 0.5$ the C_{60}—C_{70} mixtures can be supercooled down to relatively low temperatures, as it can be deduced from Fig. 7 where the locus of T versus x for which $D=10^{-5}$ cm^2/s (a value of the diffusion coefficient sufficiently low to be considered close to the lower boundary for liquid diffusive behavior) is displayed. It appears, in particular, that at $x=0.5$ the mixture is liquid down to $\simeq$1100 K.

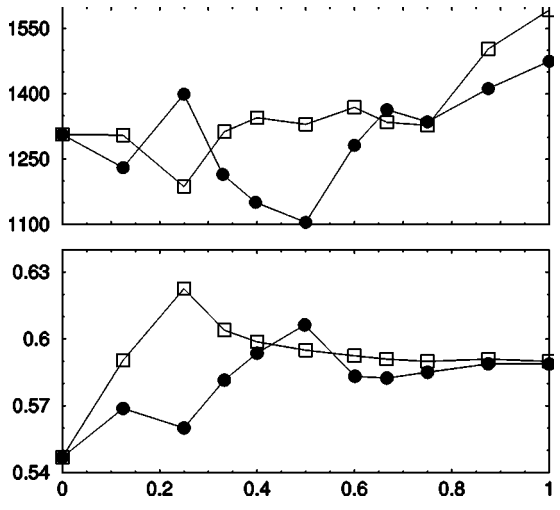

FIG. 7. Temperature (top) and total packing (bottom) values for the isodiffusivity ($D=10^{-5}$ cm^2/s) points of the C_{60}/C_{70} (circles) and C_{60}/C_{84} (squares) mixtures.

It is now instructive to compare the present results with those obtained in the investigation of HSM. To such an aim, it is worth defining a packing fraction of the mixed fullerene system, in terms of effective hard sphere diameters. We first define from $v_{ij}(r)$ a reference potential $v_{ij}^{\mathrm{ref}}(r)$ according to the well known Weeks-Chandler-Andersen prescription,[23] namely,

$$v_{ij}^{\mathrm{ref}} = \begin{cases} v_{ij}(r) + \varepsilon_{ij} & \text{if } r \leqslant r_{ij}^{\min} \\ 0 & \text{if } r > r_{ij}^{\min} \end{cases} . \tag{2}$$

where $r_{ij}^{\min}$ is the position and ϵ_{ij} the depth of the $v_{ij}(r)$ potential minimum.

Effective hard sphere diameters are then estimated according to the well known Barker and Henderson (BH) prescription:[24]

$$\sigma_{ij}^{BH} = \int_{\infty}^{0} \{1 - \exp[-\beta v_{ij}^{\mathrm{ref}}(r)]\} dr . \tag{3}$$

The total packing fraction is then defined through the formula

$$\eta = \pi/6[\rho_{C_{60}}(\sigma_{C_{60}}^{\mathrm{BH}})^3 + \rho_j(\sigma_{jj}^{\mathrm{BH}})^3]. \tag{4}$$

In the present case $\sigma_{jj}^{\mathrm{BH}}$ is the BH diameter of C_{70}. As far as the cross effective diameter $\sigma_{ij}^{\mathrm{BH}}$ is concerned, it turns out that its value determined via the application of Eq. (3) is practically within 1% of the average of the like diameters $\sigma_{ii}^{\mathrm{BH}}$. This implies that our procedure maps the fullerene mixed system onto a substantially *additive* hard sphere mixture.

As anticipated in the Introduction, significant similarities emerge between the present results and what was found in previous studies of HSM. Specifically, though we cannot determine a rigorous liquidus of the mixture, this requiring quite demanding free energy calculations, one can reasonably surmise that the iso-diffusivity curve in Fig. 7 may give a rough idea of the overall appearance of such solid-liquid coexistence curve. We note, in this instance, that the iso-D pattern for the C_{60}/C_{70} mixture has a shape similar to an eutectic coexistence line. Now, euctectic phase diagrams are found in HSM for size ratios $\alpha < 0.9$, according to Ref. 14, and for $\alpha < 0.875$, according to Ref. 17. Moreover, when an attractive van der Waals term is added to the HSM potential, DFT calculations[15] show that eutectics are already encountered at $\alpha = 0.94$. It thus emerges that the presence of an eutectic-shaped iso-D curve for the size ratio $(\sigma_{C_{60}}^{\mathrm{BH}}/\sigma_{C_{70}}^{\mathrm{BH}}) = 0.93$ (noticeably equal to the size ratio of Table I) is fully consistent with the cited DFT analysis. It also appears from Fig. 7 that in correspondence of the "eutectic" point, where the system maintains a liquidlike behavior down to relatively low temperatures, one finds a maximum of the effective packing, as well as the formation of glassy phases. Both these two features have been clearly revealed in investigations of binary colloidal hard spheres by Bartlett,[18] showing the existence of highly packed liquids in correspondence of the eutectic points, with contextual formation of colloidal glasses. We shall further comment upon this analogy when discussing mixtures of smaller size ratio than C_{60}/C_{70}.

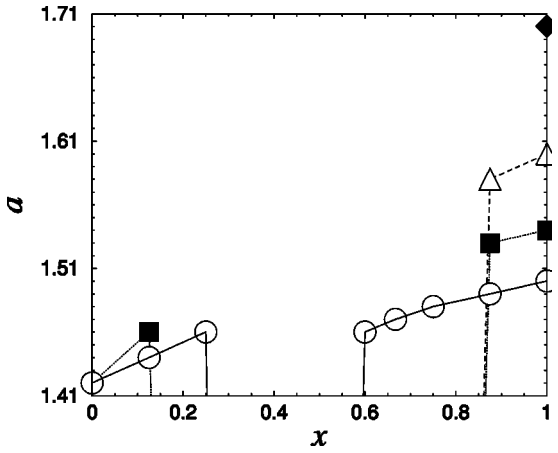

FIG. 8. RT lattice constants a (in nanometers) versus concentrations for the fullerene solid solutions: C_{60}/C_{70} (circles), C_{60}/C_{76} (squares), C_{60}/C_{84} (triangles), and C_{60}/C_{96} (diamond).

We finally note that, as shown in Fig. 8, the solid solution lattice parameter exhibits a roughly linear increasing trend over the two separate concentration ranges upon which solid solutions are formed. The two branches however do not match each other, as is clearly visible in the figure. It thus emerges a departure from Vergard's empirical rule,[25] predicting the linear increase of the lattice parameter with the concentration.

B. C_{60}/C_n fullerene-mixtures: $n = 76$, 84, and 96

Investigation of fullerene mixtures of diameter ratio smaller than C_{60}/C_{70}, reveals a rapid extension of the region where solid solution does not occur. It appears in fact that fcc substitutional alloy stability is permitted only close to the extreme concentrations $x = 0$ and $x = 1$. This clearly emerges from both Table II and Fig. 8. For C_{60}/C_{76} mixtures ($\alpha = 0.89$), for instance, we obtain solid solutions only at the symmetric concentrations $x = 0.125$ and $x = 0.875$.

When further decreasing the diameter ratio, the possibility to form a crystal of small spheres with even a very little fraction of large spheres, tends to zero. Thus, in the case of C_{60}/C_{84} ($\alpha = 0.85$), only a solid very rich in large spheres ($x = 0.875$) survives. For lower α values it becomes increasingly difficult to find a mechanically stable solid phase and in fact, when we monitor the freezing of C_{60}/C_{96} ($\alpha = 0.79$), we find that the amorphous zone extends over the entire concentration range. The emergence of a lower boundary in the size ratio for the stability of the solid solution appears in agreement with the semi-empirical Hume-Rothery rule,[26] stating that no solid solution can be formed for $\alpha < 0.85$.

As done for the C_{60}—C_{70} mixture, we make reference to HSM in order to perform a comparative analysis of size ratio effects. We reproduce in Fig. 9, for the benefit of the reader, the DFT theory results obtained in Refs. 14 and 15 for HSM with $\alpha = 0.9$ and 0.85. It clearly appears that even a moderate reduction of the size ratio has a marked influence on phase coexistence conditions. In practice, as discussed in the cited works, when $\alpha < 0.9$, the solid-liquid boundaries rise almost vertically, with most of the concentration/temperature plane

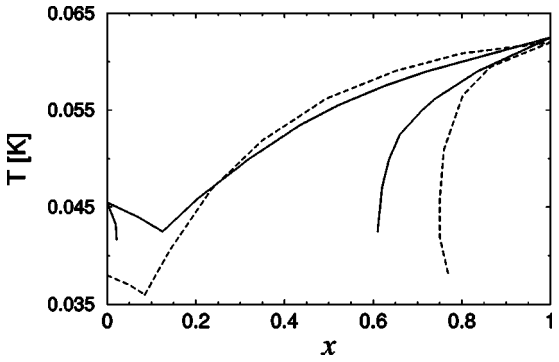

FIG. 9. Eutectic phase diagram for binary hard sphere mixtures with diameter ratio $\alpha=0.9$ (solid line) and 0.85 (dashed line). Data have been extracted from Ref. 15.

excluded from solid solution formation. The effect is more pronounced in the small spheres rich zone and, specifically, for $\alpha=0.85$ only small spheres can still be accommodated in the lattice of larger spheres, while the opposite turns out to be impossible. Such size ratio effects appear similar to what hitherto reported to happen in fullerene mixtures. In addition we note that, as shown in Fig. 7, at $\alpha=0.85$ (C_{60}/C_{84}) a shift occurs at lower concentrations of the "eutectic" minimum in the iso-*D* curve, in correspondence of which latter one also sees a sharp maximum in the effective packing. Now, a similar shift of the eutectic point toward lower concentrations is visible in Fig. 9 for the HSM case, and has been also documented to occur in model binary colloidal mixtures.[18] It is also interesting to note the fair resemblance of the η versus x pattern in C_{60}/C_{84} (see Fig. 7, bottom) as compared to the liquidus diagram for HSM at $\alpha=0.85$ reported in Fig. 8 of Ref. 17.

Our results also evidentiate an enhanced trend to glass formation (at sufficiently low temperatures) over concentration ranges which become the larger, the smaller the size ratios of the fullerene components become. This finding too appears in full agreement with the mentioned study of colloidal systems[18] in which, to quote the authors, "by correlating the enhanced fluid stability found in the eutectic region with ease of glass formation," one can "predict the composition of binary suspensions which will most readily form colloidal glasses."

In order to attempt an explanation of the emerging similarities with colloidal-like systems behavior, we recall first of all that a close analogy between the glass transition of pure C_{60}, and vitrification of colloidal suspensions or protein solutions has been highlighted in our previously quoted study.[21] As discussed in that work, the basic physical reason of such a similarity essentially resides in the short-ranged nature of the interaction potential characterizing both the fullerene-fullerene interaction in the pure C_{60} case, and the macroparticle interaction in the complex system case. Such interaction features are obviously also present also in the mixture case.

As far as the mechanism of vitrification is concerned, one can observe that colloidlike systems are often formed by particles of various size, and the effect of such polydispersity on the ordering behavior is not well understood. Several authors have recently undertaken such an investigation;[27–30] the ensuing phase diagram, however, turns out to be complicated even in the simplest case of binary hard sphere mixtures. For these latter, a simple way to select feasible candidates to form solid structures is to use packing arguments. One must recall in this instance the basic freezing mechanism of one component hard spheres: Confining the particles to lattice points lowers the configurational entropy, but increases the free volume entropy associated with local particle motion; freezing will then occur when this balance leads to an entropy gain. Now, in a binary system the effect of progressively replacing smaller spheres with larger ones, is to disorder the solid phase which quickly becomes unstable (see, e.g., the crystallization gap $0.3\leqslant x\leqslant 0.5$ in C_{60}/C_{70} mixtures). In this last case the onset of an amorphous phase through "self assembling" of smaller spheres, closely packing in the cavities between the larger ones, might be preferred to crystallization. This requirement becomes more and more stringent with the lowering of the size ratio until a threshold value is reached below which only a strongly packed glasslike disordered phase is expected to survive.

As anticipated in Sec. II, we have finally also investigated the effect of varying the cooling rate on the crystallization process, by adopting CR2 for C_{60}/C_{70}, C_{60}/C_{84}, and C_{60}/C_{96} mixtures at equimolar concentration $x=0.5$. Although the cooling is slower than previously adopted, we did not observe in any of the systems investigated the onset of crystallization, similar to what happened through the previous cooling procedure CR1. Conversely, we invariably find that for sufficiently low temperatures a glassy phase is eventually formed. When we further cool such a glassy phase down to 600 K, we do not experience any change in the amorphous nature of the formed phase.

IV. CONCLUSIONS

We have investigated through constant pressure MD simulations the behavior of super-cooled liquid and solid binary fullerene mixtures in a central pair potential description of the molecular interactions. The attention has been focused on the characterization of the phase behavior upon varying the diameter ratio in the range $0.93\geqslant\alpha\geqslant 0.79$. We find that mixtures whose components have fairly similar sizes, like C_{60} and C_{70}, are able to order in substitutionally disordered fcc lattices over a wide range of concentrations, with the exception of an intermediate region over which they arrange in a highly packed liquid phase, by eventually forming a glass at sufficiently low temperatures.

Within the limits of the adopted model, these results seem to qualitatively agree with the experimental data of Refs. 4 and 6 in which it was found only partial mutual solubility of C_{60} and C_{70}, with an intermediate concentration gap for solid solution formation. We recall, however, that the experimental evidence concerning this point is somewhat controversial (see Refs. 5–7), and a more realistic description of fullerene-fullerene interaction might be necessary, before drawing definite conclusions.

When extending our simulations to fullerene mixtures of lower diameter ratio, as, e.g., C_{60}/C_{76} or C_{60}/C_{84}, (for

which, unfortunately, no experimental evidence seems available), we observe that the intermediate amorphous region expands dramatically. Actually, we have verified that for a size ratio $\alpha=0.79$, corresponding to the C_{60}/C_{96} mixture, no solid solution can be formed over the whole concentration axis.

We have attempted an interpretation of our MD results in terms of the solid-liquid co-existence of HSM as studied by other authors.[14–17] Specifically, no tendency toward phase separation was detected in the "no solid solution" zone evidentiated in such studies[14,15] for similar size ratios as here envisaged; rather, strongly packed glasslike disordered phases were found, as encountered in model binary colloidal systems and in polystirene spheres (Refs. 18 and 19). We have discussed the similarities with such complex fluid phase behavior, by recalling an analogous result we have recently obtained in studying model pure C_{60}, where a high temperaturee glass transition is also found with features similar to those of vitrifications in colloidal suspensions and protein solutions.[21]

These circumstances prompt to a more extensive investigation of fullerene mixtures, aimed, e.g., at the determination of the glass transition temperatures and densities in the different mixtures here considered, and in general, to a more complete determination of phase diagram properties. Work in this direction is in progress.

ACKNOWLEDGMENT

One of the authors (R.R.) wishes to thank Professor E. Bruno for useful suggestions.

*Corresponding author; e-mail address: mcabramo@unime.it

[1] J. L. Sauvajol, Z. Hricha, A. Zahab, and R. Aznar, Solid State Commun. **88**, 693 (1993).
[2] K. Tanaka, T. Sato, T. Yamabe, K. Yoshizawa, K. Okahara, and A. A. Zakhidov, Phys. Rev. B **51**, 990 (1995).
[3] A. R. McGhie, J. E. Fischer, P. A. Heiney, P. W. Stephens, R. L. Cappelletti, D. A. Neumann, W. H. Mueller, H. Mohn, and H. U. Termeer, Phys. Rev. B **49**, 12 614 (1994); P. Zielinski, W. Schranz, D. Havlik, and A. V. Kityk, Eur. Phys. J. B **24**, 155 (2001).
[4] M. S. Baba, T. S. L. Narasimhan, R. Balasubramanian, N. Sivaraman, and C. K. Mathews, J. Phys. Chem. **98**, 1333 (1994).
[5] K. Kniaz, J. E. Fischer, L. A. Girifalco, A. R. McGhie, R. M. Strongin, and A. B. Smith III, Solid State Commun. **96**, 739 (1995).
[6] D. Havlik, W. Schranz, M. Haluska, H. Kuzmany, and P. Rogl, Solid State Commun. **104**, 775 (1997).
[7] W. Sekkal, H. Aourag, and M. Certier, Phys. Lett. A **251**, 132 (1999).
[8] L. F. Girifalco, J. Phys. Chem. **95**, 5370 (1991); **96**, 858 (1992).
[9] A. Cheng, M. L. Klein, and C. Caccamo, Phys. Rev. Lett. **71**, 1200 (1993); D. Costa, G. Pellicane, M. C. Abramo, and C. Caccamo, J. Chem. Phys. **118**, 304 (2003).
[10] M. C. Abramo and C. Caccamo, J. Phys. Chem. Solids **57**, 1751 (1996).
[11] M. C. Abramo, C. Caccamo, D. Costa, and G. Pellicane, Europhys. Lett. **54**, 468 (2001).
[12] F. Micali, M. C. Abramo, and C. Caccamo, J. Phys. Chem. Solids **64**, 319 (2003).
[13] V. I. Zubov, Mol. Mater. **13**, 385 (2000).
[14] J. L. Barrat, M. Baus, and J. P. Hansen, Phys. Rev. Lett. **56**, 1063 (1986).
[15] J. L. Barrat, M. Baus, and J. P. Hansen, J. Phys. C **20**, 1413 (1987).
[16] X. C. Zeng and David W. Oxtoby, J. Chem. Phys. **93**, 4357 (1990).
[17] W. G. T. Kranendonk and D. Frenkel, J. Phys.: Condens. Matter **1**, 7735 (1989); Mol. Phys. **72**, 679 (1991).
[18] P. Bartlett, J. Phys.: Condens. Matter **2**, 4979 (1990).
[19] W. H. Shih and D. Stroud, J. Chem. Phys. **80**, 4429 (1984).
[20] D. Turnbull, J. Physiol. Paris **35**, C4-1, (1974); X. P. Tang, U. Geyer, R. Busch, W. L. Jonshon, and Y. Wu, Nature (London) **402**, 160 (1999).
[21] M. C. Abramo, C. Caccamo, D. Costa, and R. Ruberto, J. Phys. Chem. B **108**, 13576 (2004).
[22] F. Gugenberger, R. Heid, C. Meingast, P. Adelmann, M. Braun, H. Wuhl, M. Haluska, and H. Kuzmany, Phys. Rev. Lett. **69**, 3774 (1992);. T. Matsuo, T. Tsuo, H. Suga, W. I. F. David, R. M. Ibberson, P. Benrier, A. Zahab, C. Fabre, A. Rassat, and A. Dworkin, Solid State Commun. **83**, 711 (1992).
[23] J. D. Weeks, D. Chandler, and H. C. Andersen, J. Chem. Phys. **54**, 5237 (1971).
[24] J. A. Barker and D. Henderson, J. Chem. Phys. **47**, 2856 (1967).
[25] See, e.g., *Modern Crystallography II*, edited by D. K. Wainshtein (Springer-Verlag, Berlin, 1982), p. 116.
[26] W. Hume-Rothery, R. E. Smallman, and C. W. Haworth, *The Structure of Metals and Alloys* (The Metals and Metallurgy Trust, London, 1969).
[27] P. Bartlett and P. B. Warren, Phys. Rev. Lett. **82**, 1979 (1999).
[28] D. A. Kofke and P. G. Bolhuis, Phys. Rev. E **59**, 618 (1999).
[29] H. Xu and M. Baus, Phys. Rev. E **61**, 3249 (2000); J. Chem. Phys. **118**, 5045 (2003).
[30] N. B. Wilding and P. Sollich, J. Chem. Phys. **116**, 7116 (2002).